Acta Crystallographica Section D
Biological Crystallography
ISSN 1399-0047

Kinase crystal identification and ATP-competitive inhibitor screening using the fluorescent ligand SKF86002

Lorien J. Parker,[a] Shigenao Taruya,[a] Keiko Tsuganezawa,[a,b] Naoko Ogawa,[a,b] Junko Mikuni,[a,b] Keiko Honda,[a,b] Yuri Tomabechi,[a,b] Noriko Handa,[a] Mikako Shirouzu,[a,b] Shigeyuki Yokoyama[a,c] and Akiko Tanaka[a,b]*

[a]Systems and Structural Biology Center, RIKEN, 1-7-22 Suehiro-cho, Tsurumi, Yokohama 230-0045, Japan, [b]Center for Life Science Technologies, RIKEN, 1-7-22 Suehiro-cho, Tsurumi, Yokohama 230-0045, Japan, and [c]Structural Biology Laboratory, RIKEN, 1-7-22 Suehiro-cho, Tsurumi, Yokohama 230-0045, Japan

Correspondence e-mail: aktanaka@riken.jp

Received 26 August 2013
Accepted 17 October 2013

PDB references: Pim1–SKF86002, 4ll5; Pim1–quercetin, 4lmu; Pim1–compound **1**, 4lm5; HCK–SKF86002, 4lud; HCK–A-419259, 4lue

The small kinase inhibitor SKF86002 lacks intrinsic fluorescence but becomes fluorescent upon binding to the ATP-binding sites of p38 mitogen-activated protein kinase (p38α). It was found that co-crystals of this compound with various kinases were distinguishable by their strong fluorescence. The co-crystals of SKF86002 with p38α, Pim1, ASK1, HCK and AMPK were fluorescent. Addition of SKF86002, which binds to the ATP site, to the co-crystallization solution of HCK promoted protein stability and thus facilitated the production of crystals that otherwise would not grow in the apo form. It was further demonstrated that the fluorescence of SKF86002 co-crystals can be applied to screen for candidate kinase inhibitors. When a compound binds competitively to the ATP-binding site of a kinase crystallized with SKF86002, it displaces the fluorescent SKF86002 and the crystal loses its fluorescence. Lower fluorescent signals were reported after soaking SKF86002–Pim1 and SKF86002–HCK co-crystals with the inhibitors quercetin, a quinazoline derivative and A-419259. Determination of the SKF86002–Pim1 and SKF86002–HCK co-crystal structures confirmed that SKF86002 interacts with the ATP-binding sites of Pim1 and HCK. The structures of Pim1–SKF86002 crystals soaked with the inhibitors quercetin and a quinazoline derivative and of HCK–SKF86002 crystals soaked with A-419259 were determined. These structures were virtually identical to the deposited crystal structures of the same complexes. A KINOME*scan* assay revealed that SKF86002 binds a wide variety of kinases. Thus, for a broad range of kinases, SKF86002 is useful as a crystal marker, a crystal stabilizer and a marker to identify ligand co-crystals for structural analysis.

1. Introduction

Protein kinases play critical roles in cellular signal transduction pathways and are often involved in disease states. Determination of the three-dimensional structures of these kinases, and of their interactions with ligands and inhibitors, contributes vital information about how these proteins perform their biological functions, and often provides insights into the molecular bases of diseases. In addition, such protein–ligand structures represent an ideal starting point for inhibitor development for therapeutic purposes.

One of the initial hurdles in X-ray crystallographic studies is identifying the conditions that produce crystal growth. In many cases, crystallization drops contain numerous unidentifiable objects as well as precipitation, phase separation,

microcrystals and salt crystals. The identification of the initial conditions that yield actual protein crystals is rarely straightforward and is thus a time-, material- and cost-consuming process. Even after promising conditions have been identified, the material of the 'crystal' still needs to be established, as it is often difficult to differentiate between protein and salt crystals. Many different methods are available for distinguishing between salts and proteins prior to a diffraction check. Such methods include inspecting the crystal with a polarizing filter, testing the solidity of the crystal by crushing it or even exposing it to extreme heat to see if it will 'melt'. Although all of these methods have their individual merits, their drawbacks, including ambiguity, cost, time and variations owing to user interpretation or protein composition, often make it difficult to draw confident conclusions. A diffraction check is almost totally conclusive, but may be misleading if the protein crystal diffracts to very low resolution.

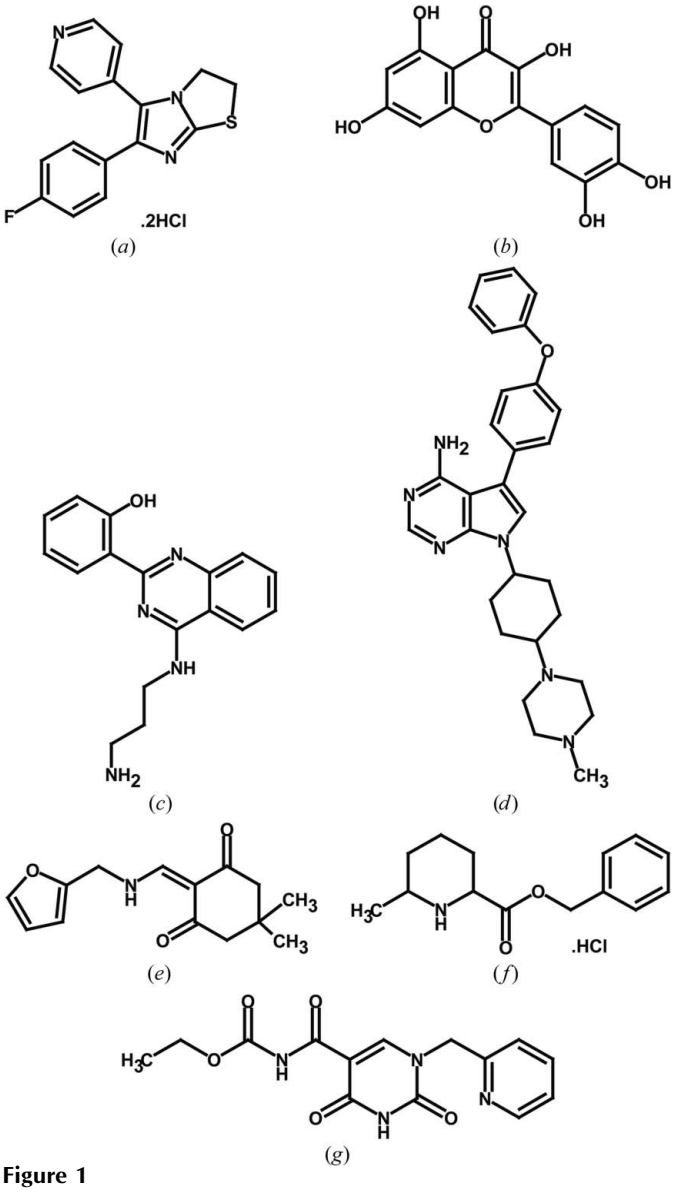

Figure 1
Chemical structures. The chemical structures of the compounds (*a*) SKF86002 dihydrochloride, (*b*) quercetin, (*c*) compound **1**, (*d*) A-419259, (*e*) P-017529, (*f*) P-020547 and (*g*) P-043305.

During the last decade, fluorescence techniques have been shown to be effective in the identification of protein crystals. Examples of such techniques include the use of intrinsic protein fluorescence (Judge *et al.*, 2005) or covalent protein modification (Forsythe *et al.*, 2006). Forsythe and coworkers labelled a protein using the visible fluorescent probe carboxyrhodamine succinimidyl ester to identify optimal conditions for protein crystallization. Encouragingly, the presence of small amounts of the label was not detrimental to the quality of the X-ray diffraction data. However, the method was not simple, as it required additional purification steps after labelling to remove the unreacted protein or reagent. Alternatively, Groves and coworkers explored the possibility of labelling proteins with 1-anilinonaphthalene-8-sulfonic acid (1,8-ANS), which lacks intrinsic fluorescence but becomes fluorescent upon interaction with hydrophobic sites in proteins (Groves *et al.*, 2007). However, the protein-labelling protocol suffers from the problem that this dye binds proteins nonspecifically.

Although many techniques to facilitate protein crystal identification have been investigated, only a few have the potential for use in subsequent stages in the drug-discovery process. In addition, many existing techniques that are used to identify protein crystals, such as dye soaking, the click-test, a diffraction check *etc.*, can render the crystal unusable for further experimentation.

Here, we have developed a method that uses a compound, SKF86002, to assist in identifying kinase crystals by fluorescence and in screening new kinase inhibitors. This relatively straightforward process simply involves incubating the protein with the water-soluble compound SKF86002 dihydrochloride prior to crystallization. The resulting protein co-crystals are fluorescent, which makes them easily identifiable. The crystals can then be immediately utilized for inhibitor-screening experiments. If the compound screening is successful, then this is indicated by the loss of the fluorescent signal of the crystal owing to the displacement of SKF86002 by the competitive binding of a compound. The resulting soaked crystal can then be used for data collection. We show in this paper that the information gained from the crystal structures of these soaked complexes is useful for structure-guided drug-design studies.

SKF86002 {6-(4-fluorophenyl)-2,3-dihydro-5-(4-pyridinyl)-imidazo[2,1-*b*]thiazole; Fig. 1*a*} is a small bicyclic imidazole (Lantos *et al.*, 1984). It was subsequently identified as an inhibitor of p38 mitogen-activated protein kinase (p38α; Gallagher *et al.*, 1997). Upon binding to the ATP-binding site of p38α, it generated fluorescence (Pargellis *et al.*, 2002). Here, we report that SKF86002 binds not only p38α but also a wide variety of kinases. SKF86002 thus represents a powerful tool for the identification of kinase crystals and is applicable as a probe to screen for compounds that bind competitively to the ATP-binding site. Furthermore, we show that the SKF86002 co-crystals soaked with potential inhibitors can be used directly for data collection, thus providing useful information for further inhibitor design and optimization.

2. Materials and methods

2.1. Protein cloning, expression and purification

2.1.1. p38α. The full-length *p38α* gene was PCR-amplified using the human *p38α2* cDNA clone (RefSeq accession No. NM_139012.2) as the template. After amplification of the target gene by forward 5′-CAGTACTCGAGATGTCTCAGGAGAGGCCCAC-3′ and reverse 5′-CTTAAGGATCCCTAGGACTCCATCTCTTCTTGGTC-3′ primers, it was cloned into the pET-15b vector (Novagen, Darmstadt, Germany), encoding a polypeptide with an N-terminal hexahistidine tag to facilitate purification. Site-directed mutagenesis (D176A and F327S) was performed on the p38α gene cloned in the pET-15b vector using the QuikChange II XL Site-Directed Mutagenesis Kit (Stratagene, La Jolla, California, USA). The p38$\alpha^{D176A,F327S}$ mutant is in a constitutively active state and maintains all of the biochemical and pharmacological properties of active p38α (Diskin *et al.*, 2007).

The p38$\alpha^{D176S,F327S}$ protein was expressed in *Escherichia coli* BL21(DE3)pLysS cells. The cells were grown at 303 K, induced with 0.3 m*M* isopropyl β-D-1-thiogalactopyranoside (IPTG) and cultured for a further 5 h at 303 K. The cells were harvested and suspended in buffer *A* [50 m*M* Tris–HCl pH 8.0, 500 m*M* NaCl, 10 m*M* imidazole, 0.3 mg ml^{-1} lysozyme, 75 µg ml^{-1} DNase, 75 µg ml^{-1} RNase and cOmplete Protease Inhibitor Cocktail (Roche Applied Science, Germany)]. The cell suspension was disrupted by passage through a French pressure cell (SLM Aminco, Irvine, California, USA) at a pressure of 20.7 MPa. The obtained lysate was centrifuged and the supernatant was loaded onto a HisTrap HP column (GE Healthcare, Fairfield, Connecticut, USA). The p38$\alpha^{D176S,F327S}$ protein was eluted with a linear gradient of 10–500 m*M* imidazole in buffer *B* (50 m*M* Tris–HCl pH 8.0, 500 m*M* NaCl). The His tag of the protein was cleaved by thrombin digestion overnight at 277 K. The mixture was desalted on a HiPrep 26/60 Desalting column (GE Healthcare) and was then passed through a second HisTrap HP column. The p38$\alpha^{D176S,F327S}$ protein containing an N-terminal artificial Gly-Ser-His-Met-Leu-Glu sequence was obtained. After the protein solution had been desalted, it was subsequently loaded onto a HiTrap Q HP column (GE Healthcare) and the bound protein was eluted with a linear gradient of 20–1000 m*M* NaCl in buffer *C* (20 m*M* Tris–HCl pH 8.0). The obtained protein fraction was concentrated and the buffer was exchanged to buffer *D* [10 m*M* HEPES pH 7.4, 150 m*M* NaCl, 2 m*M* dithiothreitol (DTT)] using an Amicon Ultra-15 10 000 molecular-weight cutoff centrifugal filter (Millipore, Billerica, Massachusetts, USA). The total protein concentration was determined using the Bio-Rad protein-assay reagent (Bio-Rad, Hercules, California, USA). The purity of the protein was assessed by sodium dodecyl sulfate polyacrylamide gel electrophoresis (SDS–PAGE) and it was found to be nearly homogeneous.

2.1.2. Pim1. Preparation of the kinase domain (residues 29–313) of human Pim1 for structural determination and soaking/bleaching experiments was performed as reported by Tsuganezawa *et al.* (2012). The purified Pim1 was concentrated to 10 mg ml^{-1} in 20 m*M* Tris–HCl buffer pH 8.0 containing 200 m*M* NaCl, 2 m*M* $CaCl_2$, 2 m*M* $MgCl_2$ and 5 m*M* DTT for crystallization.

2.1.3. ASK1. The DNA fragment encoding ASK1 (646–940) (including the kinase domain Asn680–Leu938) was PCR-amplified using the human *ASK1* cDNA clone (RefSeq accession No. NP_005914.1) as the template (Bunkoczi *et al.*, 2007). After amplification of the target gene using forward 5′-GGGATGCGGGCATATGCAGGATCCGTTTTTTGAGATGGTGAAC-3′ and reverse 5′-GGGATGCGGGCTCGAGTCGACTTATCAAACTTTTAAAAACTCATC-3′ primers, the PCR-amplified gene was cloned into the pCold TF DNA vector (Takara, Kyoto, Japan), encoding a polypeptide with an N-terminal hexahistidine tag. The ASK1 (646–940) protein was expressed in *E. coli* BL21 Star (DE3) cells. The cells were grown at 310 K and were induced by 0.5 m*M* IPTG for an additional 24 h at 303 K. The cells were harvested, disrupted, purified on a HisTrap HP column and desalted in the same manner as the p38$\alpha^{D176S,F327S}$ protein. The His tag was cleaved by treatment with HRV 3C protease overnight at 277 K. The His-tag-cleaved ASK1 (646–940) protein containing an N-terminal artificial Gly-Pro-Ser-Ala-Gly-Leu-Val-Pro-Arg-Gly-Ser-Gly-Gly-Ile-Glu-Gly-Arg-His-Met-Glu-Asp-Pro sequence was purified by chromatography on a second HisTrap HP column, a HiTrap Q HP column and a Mono Q 5/50 GL column and by gel filtration on a HiLoad 16/60 Superdex 75 pg column (GE Healthcare). The protein solution was concentrated and stored in buffer *D* (10 m*M* HEPES pH 7.4 containing 150 m*M* NaCl and 2 m*M* DTT) in the same manner as the p38$\alpha^{D176S,F327S}$ protein.

2.1.4. HCK. The SH3-SH2-kinase domain region of human HCK was prepared as described previously (Saito *et al.*, 2013). We changed amino-acid residues 523–525 (Gln-Gln-Gln) to Glu-Glu-Ile to produce the HCKQQQ523EEI mutant protein reported previously (PDB entry 1qcf; Schindler *et al.*, 1999). The purity of the protein in 20 m*M* Tris–HCl buffer pH 8.0 containing 150 m*M* NaCl, 10% glycerol and 3 m*M* DTT was greater than 98% as judged by SDS–PAGE.

2.1.5. AMPK. The kinase domain (residues 6–279) of the human AMPKα2^{T172D} mutant was prepared as described previously (Handa *et al.*, 2011), with an additional purification step using a HisTrap column (GE Healthcare) to separate the AMPKα from the uncleaved protein and the TEV protease before the gel-filtration step. The AMPKα2^{T172D} mutant protein containing an N-terminal artificial Gly-Ser sequence was concentrated to 5 mg ml^{-1} in 20 m*M* Tris–HCl buffer pH 8.5 containing 300 m*M* NaCl, 10% glycerol and 2 m*M* DTT for crystallization.

2.2. Chemicals

The SKF86002 dihydrochloride {6-(4-fluorophenyl)-2,3-dihydro-5-(4-pyridinyl)imidazo[2,1-*b*]thiazole dihydrochloride} used for crystallization was purchased from Tocris Bioscience (Bristol, England), while the SKF86002 {6-(4-fluorophenyl)-2,3-dihydro-5-(4-pyridinyl)imidazo[2,1-*b*]thiazole} used for the kinome dendrogram was from Sigma–Aldrich (St Louis,

Table 1
Data-collection and refinement statistics.

Values in parentheses are for the highest resolution shell.

	Pim1–SKF86002	Pim1–quercetin	Pim1–compound **1**	HCK–SKF86002	HCK–A-419259
Data collection					
Temperature (K)	100	100	100	100	100
Space group	$P6_1$	$P6_5$	$P6_5$	$P2_1$	$P2_12_12_1$
Unit-cell parameters					
a (Å)	98.65	97.42	97.68	48.30	73.40
b (Å)	98.65	97.42	97.68	73.40	73.40
c (Å)	80.27	80.58	80.78	180.29	181.49
α (°)	90	90	90	90	90
β (°)	90	90	90	96.77	90
γ (°)	120	120	120	90	90
Resolution range (Å)	42.72–2.00 (2.06–2.00)	48.71–2.38 (2.53–2.38)	29.73–2.25 (2.35–2.25)	47.76–2.85 (2.94–2.85)	46.77–3.04 (3.16–3.04)
Completeness (%)	99.43 (98.9)	100 (100)	100 (100)	99.9 (99.9)	99.81 (99.6)
No. of observations	333897 (49094)	89474 (12877)	469376 (66932)	112600 (16365)	174049 (24488)
No. of unique reflections	29928 (4334)	17553 (2549)	20902 (3024)	29538 (4274)	24812 (3549)
$R_{\rm merge}$	0.115 (0.40)	0.073 (0.37)	0.066 (0.41)	0.082 (0.41)	0.108 (0.37)
$\langle I/\sigma(I)\rangle$	3.7 (1.9)	6.3 (2.1)	9.8 (1.8)	6.5 (1.9)	5.7 (1.9)
Multiplicity	11.2 (11.3)	5.1 (5.1)	22.5 (22.1)	3.8 (3.8)	7.0 (6.9)
Refinement					
No. of non-H atoms					
Total	2413	2268	2308	6749	6814
Compound	21	22	22	21	36
Solvent (H_2O)	195	80	111	210	26
$R_{\rm work}$ (%)	16.82 (19.06)	17.00 (20.88)	15.57 (16.67)	21.23 (29.37)	20.54 (24.37)
$R_{\rm free}$ (%)	18.94 (24.56)	20.44 (27.51)	19.79 (22.12)	26.07 (36.73)	25.62 (29.00)
No. of reflections	29915 (2592)	17522 (2743)	20872 (2445)	29497 (2514)	24715 (2561)
R.m.s.d.s from ideal geometry					
Bonds (Å)	0.003	0.004	0.013	0.002	0.003
Angles (°)	0.702	0.768	1.266	0.622	0.646
Mean B (Å^2)					
Protein	36.62	56.63	39.83	69.41	71.21
Compound	42.20	55.77	34.91	56.77	43.30
Ramachandran plot					
Residues in favoured regions (%)	98.87	98.96	98.85	96.91	96.72
Outliers (%)	0	0	0	0.12	0.24
PDB code	4ll5	4lmu	4lm5	4lud	4lue

Missouri, USA). Quercetin and compound **1** {2-[4-(3-aminopropylamino)quinazolin-2-yl]phenol} were purchased from Tokyo Chemical Industry Co. Ltd (Tokyo, Japan) and InterBioScreen Ltd (Moscow, Russia), respectively. A-419259 was a kind gift from Dr Y. Hashizume (RIKEN). P-017529 and P-020547 were purchased from ChemBridge Corp. (San Diego, California, USA) and P-043305 was purchased from Maybridge Chemical Co. Ltd (Cambridge, England). The structures of these compounds are shown in Fig. 1. The compounds, with the exception of SKF86002 dihydrochloride, were dissolved in DMSO and stored at 253 K.

The IC_{50} values of SKF86002 towards the kinases Pim1, HCK and AMPK were investigated by kinase Glo assays and kinase mobility shift assays as described previously (Tsuganezawa *et al.*, 2012).

2.3. Crystallization with SKF86002

A 16 mg ml^{-1} solution of p38α was mixed with an equal volume of 3 m*M* SKF86002 dihydrochloride and was co-crystallized using the Crystal Screen reagent set (Hampton Research, Aliso Viejo, California, USA) at 293 K.

ASK1 concentrated to 19 mg ml^{-1} was mixed with a final concentration of 1.5 m*M* SKF86002 dihydrochloride and co-crystallized using the Crystal Screen reagent set (Hampton Research).

Pim1 concentrated to 10 mg ml^{-1} was incubated with 2 m*M* SKF86002 dihydrochloride overnight. It produced exquisite fluorescent crystals under many conditions from the PACT (Molecular Dimensions, Suffolk, England) and Index (Hampton Research) screens. The crystals used for data collection for the SKF86002 and quercetin complexes were both grown in 0.2 *M* potassium/sodium tartrate, 0.1 *M* bis-tris propane pH 7.5, 20%(*w*/*v*) PEG 3350. The crystals were cryocooled in well solution containing 20% glycerol. For comparison and as a control experiment, Pim1 apo crystals grown in 100 m*M* citrate buffer pH 5.5 containing 200 m*M* NaCl and 1 *M* $(NH_4)_2HPO_4$ were also tested for fluorescence and showed no signal. These were then transferred into well solution containing 1 m*M* SKF86002 dihydrochloride to determine whether soaking could generate a signal. These crystals became fluorescent within just 10 min. They were harvested, cryoprotected with 20% glycerol and cryocooled for data collection for structural confirmation that the SKF86002 compound had bound as expected.

AMPK concentrated to 5 mg ml^{-1} was incubated with 2 m*M* SKF86002 dihydrochloride. The complex crystallized under numerous conditions. These crystals were always small

thin rectangles or flat thin plates and were not suitable for data collection.

HCK concentrated to 5 mg ml^{-1} was incubated with 2 m*M* SKF86002 dihydrochloride. It crystallized under conditions consisting of 100 m*M* Tris–HCl buffer pH 7.4–8.0, 90–100 m*M* calcium acetate, 18–20% glycerol, 20–22%(*w*/*v*) PEG 8000 at 288 K. The additive 1,5-diaminopentane dihydrochloride (Hampton Research) was added to the protein to 3%(*w*/*v*) just prior to crystallization setup. The resulting needle-like crystals were then used for streak-seeding, which subsequently produced large diamond-shaped crystals for the soaking and data-collection experiments under the conditions described below. A portion of 1 µl protein [10 mg ml^{-1} solution in 20 m*M* Tris–HCl buffer pH 8.0 containing 200 m*M* NaCl, 3 m*M* DTT, 2 m*M* SKF86002 and 3%(*w*/*v*) 5-diaminopentane dihydrochloride] was mixed with an equal volume of reservoir solution consisting of 100 m*M* Tris–HCl buffer pH 8.0, 200 m*M* calcium acetate, 10% glycerol, 12%(*w*/*v*) PEG 6000 and seeded immediately. The crystals were cryoprotected with well solution containing 30% glycerol and 3 m*M* SKF86002 dihydrochloride and were cryocooled in a nitrogen stream prior to being plunged into liquid nitrogen.

In all cases, the protein–SKF86002 dihydrochloride solution was filtered using 0.22 µm Ultrafree-MC centrifugal filter devices (Merck Millipore, Darmstadt, Germany) prior to crystallization to remove any precipitate. All crystals were grown by the hanging-drop vapour-diffusion method, except for those of p38α, ASK1 and HCK, which were grown by the sitting-drop vapour-diffusion method. All SKF86002–kinase co-crystals were observed using an AxioPlan 2 microscope (Zeiss) with epifluorescence optics. Fluorescence was detected using Zeiss filter set 01, with BP 365/12, FT 395 and LP 397 filters (an excitation filter at 365 nm, a beam-splitting mirror at 395 nm and an excitation barrier filter at 397 nm). Digital images were captured using a digital camera at a shutter speed of either 1/100 or 1/200 s.

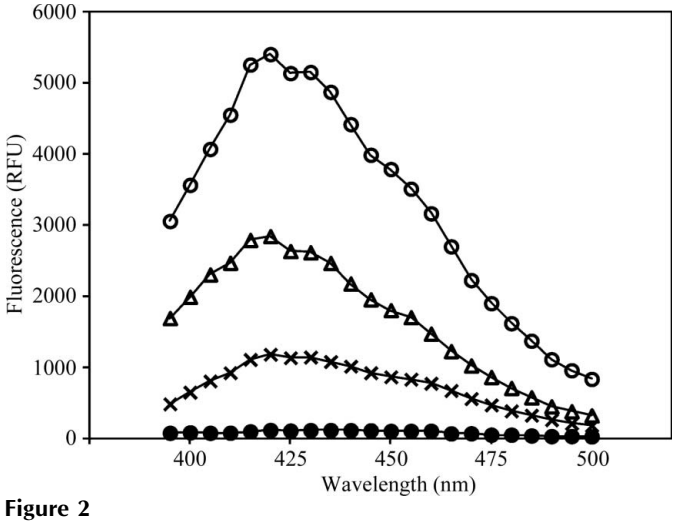

Figure 2
Fluorescence spectra of SKF86002–kinase complexes. Fluorescence spectra of 100 µ*M* SKF86002 dihydrochloride with or without each kinase. The excitation wavelength was 340 nm. Filled circles: 100 µ*M* SKF86002 dihydrochloride in 20 m*M* Tris–HCl buffer pH 8.5 containing 300 m*M* NaCl, 2 m*M* DTT and 10% glycerol. Crosses: 100 µ*M* SKF86002 dihydrochloride and 10 µ*M* Pim1 in 50 m*M* Tris–HCl buffer pH 8.0 containing 150 m*M* NaCl and 1 m*M* EDTA. Triangles: 100 µ*M* SKF86002 dihydrochloride and 10 µ*M* AMPK in 20 m*M* Tris–HCl buffer pH 8.5 containing 300 m*M* NaCl, 2 m*M* DTT and 10% glycerol. Unfilled circles: 100 µ*M* SKF86002 dihydrochloride and 10 µ*M* HCK in 20 m*M* Tris–HCl buffer pH 8.0 containing 150 m*M* NaCl, 2 m*M* DTT and 10% glycerol.

2.4. Soaking of kinase–SKF86002 co-crystals with inhibitors

Pim1–SKF86002 and HCK–SKF86002 co-crystals were transferred into fresh drops of well solution and then soaked with approximately 1–2 m*M* inhibitor with a final concentration of 10% DMSO.

2.5. Structure determination

For comparison, two data sets for Pim1–SKF86002 were collected: one from an apo crystal soaked with SKF86002 and one from a Pim1–SKF86002 co-crystal. Data from the soaked complex were collected in-house on an R-AXIS VII imaging-plate detector (Rigaku, Tokyo, Japan), while those for the co-crystallized Pim1–SKF86002 complex were collected on the microcrystallography beamline (MX2) at the Australian synchrotron. These resulted in identical structures, so only the co-crystallized data are presented here. Two data sets were also collected for Pim1 crystals soaked with two different inhibitors: one from a crystal soaked with solid compound **1** and another from crystals soaked with DMSO-dissolved quercetin. The data for the Pim1–compound **1** structure were collected in-house, while those for the Pim1–quercetin complex were collected on beamline BL26B2 at SPring-8.

Data for the HCK–SKF86002 co-crystals and those subsequently soaked with A-419259 were collected on BL26B2 at SPring-8.

All data were processed with *MOSFLM* and scaled with *SCALA*. The phases were determined by molecular replacement with *Phaser* (McCoy *et al.*, 2007), using the coordinates of Pim1 (PDB entry 3umw; Nakano *et al.*, 2012) or HCK (PDB entry 2c0t; Burchat *et al.*, 2006) as the search model. The models were built and corrected with *Coot* (Emsley & Cowtan, 2004) and refinement was performed with *PHENIX* (Adams *et al.*, 2010). The model-building and refinement statistics are summarized in Table 1. A Ramachandran plot was calculated using *PROCHECK* (Laskowski *et al.*, 1993). The data have been deposited in the PDB as entries 4ll5, 4lmu, 4lm5, 4lud and 4lue for the structures of Pim1–SKF86002, Pim1–quercetin, Pim1–compound **1**, HCK–SKF86002 and HCK–A-419259, respectively.

2.6. Kinome dendrogram

The kinome dendrogram was determined with an 800 µ*M* concentration of SKF86002. Kinase data were generated using the *scan*EDGE^{SM} kinase assay panel, which includes 97 kinases (DiscoveRx Bioscience, Fremont, California, USA), using the KINOME*scan* technology (Fabian *et al.*, 2005; Anastassiadis *et al.*, 2011). Briefly, to evaluate the interaction strength of a test compound with a target kinase, the amounts of the kinase that bound to the kinase active-site-directed

ligands immobilized on a chip were measured in the presence of the test compound.

3. Results

3.1. Labelling kinase crystals

Upon binding to the ATP-binding site of p38α, SKF86002, a small compound, reportedly became fluorescent (Pargellis *et al.*, 2002). It binds within the ATP pocket of the kinase. We found that SKF86002 binds not only p38α but also a wide variety of other kinases. Representative fluorescence spectra of the SKF86002–Pim1, SKF86002–HCK and SKF86002–AMPK complexes are shown in Fig. 2. As shown in Fig. 2, SKF86002 itself does not have any fluorescent signal, but becomes fluorescent upon binding to the ATP sites of these kinases.

Screening for co-crystallization conditions of p38α, ASK1, Pim1, AMPK and HCK with SKF86002 produced various crystal forms (Figs. 3*a*–3*h*, left panels). All of the co-crystals were distinguished by blue-white fluorescence upon exposure to UV light (Figs. 3*a*–3*h*, right panels). For reference, a salt crystal was also observed under visible light, but displayed no fluorescence (Fig. 3*i*). We were able to clearly identify the protein crystals in drops where crystals are often difficult to discern under visible light, such as drops with precipitate (Fig. 3*a*) or with crystals lying on their edge (Fig. 3*b*). Even in drops that contained surrounding precipitate that also produced a background fluorescent signal, as in Figs. 3(*a*), 3(*c*) and 3(*e*), the protein crystals were still easily and clearly visible and very well defined. In addition, small microcrystals,

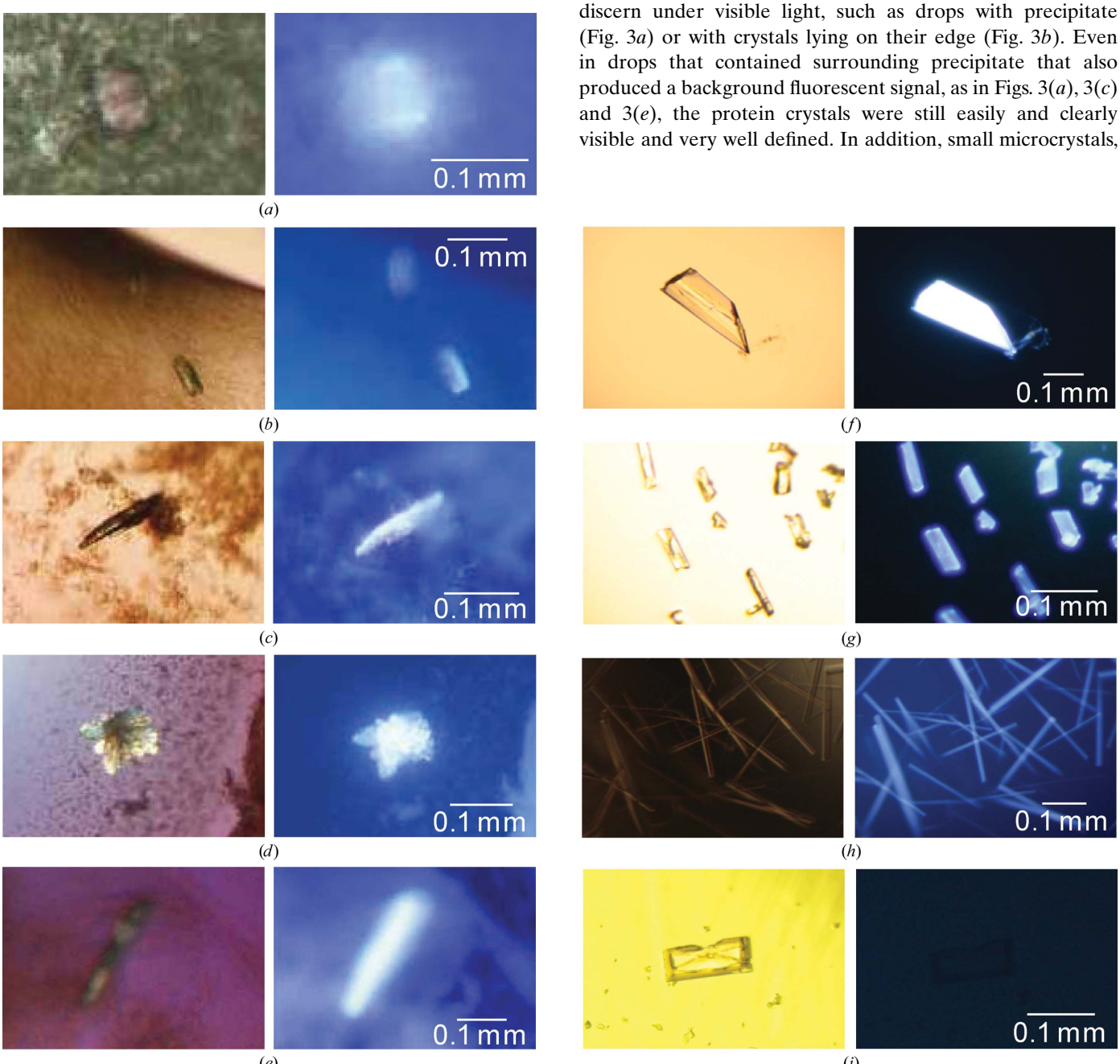

Figure 3
Fluorescence of kinase crystals with SKF86002. Left panels, white-light images; right panels, corresponding images under UV illumination. (*a*)–(*c*) p38α, (*d*, *e*) ASK1, (*f*) Pim1, (*g*) AMPK, (*h*) HCK and (*i*) salt.

such as those in Figs. 3(*c*), 3(*d*) and 3(*e*), were more clearly detectable under UV light than visible light.

Notably, SKF86002 contained in the co-crystallization solution may bind to the kinase ATP site, promote protein stability and thus assist in the production of crystals. In the case of HCK, we and another group (Sicheri *et al.*, 1997) were unable to grow crystals of the apo form. However, the complex formed with SKF86002 produced suitable crystals for analysis and data collection (Fig. 3*h*).

Furthermore, a Pim1 apo crystal lacking fluorescence was easily stained by SKF86002. By soaking this non-fluorescent apo crystal with 0.5 m*M* SKF86002 dihydrochloride, the typical blue-white fluorescent signal was rapidly observed and its intensity increased proportionally with the soaking time (Fig. 4).

3.2. Screening kinase inhibitors

Since SKF86002 binds to the kinase ATP site in crystals, it may be displaced by compounds that bind more strongly to the same ATP site and the crystals would lose their SKF86002-dependent fluorescence. This change could thus be utilized to screen for new kinase inhibitors. To test this hypothesis, Pim1–SKF86002 co-crystals were soaked with 1 m*M* quercetin, which is known to bind strongly to the Pim1 ATP-binding site (PDB entry 2o3p; Holder *et al.*, 2007). The fluorescence intensity of the crystal soaked with quercetin decreased with time (Fig. 5*a*). The Pim1–SKF86002 crystals were also soaked with a strong inhibitor, compound **1** {2-[4-(3-aminopropylamino)quinazolin-2-yl]phenol}, which was identified in our previous screening experiment (Tsuganezawa *et al.*, 2012). The crystals soaked in compound **1** dissolved in DMSO also lost their blue-white fluorescence (Fig. 5*b*).

To determine whether this screening method can be used with other kinases, the HCK co-crystals were soaked with the potent inhibitor A-419259 (Pene-Dumitrescu *et al.*, 2008). As observed for Pim1, the intensity of the fluorescent signal decreased after the addition of the inhibitor (Fig. 5*c*).

The IC_{50} values of quercetin and compound **1** for Pim1 were 55 and 150 n*M*, respectively (Tsuganezawa *et al.*, 2012), and that of A-419259 for HCK was 0.43 n*M* (Saito *et al.*, 2013). A-419259 has a much higher affinity for the kinase. The rate of bleaching for different kinases may be dependent not only on the affinity of SKF86002 *versus* that of the inhibitor, but also on the size and thickness of the crystal. The HCK crystals, for example, were thinner and tended to lose their fluorescence very quickly, while the large thick crystals of Pim1 lost their fluorescence more gradually (Figs. 5*a*, 5*b* and 5*c*).

To ensure that the loss of the fluorescent signal is owing to displacement of SKF86002 resulting from competitive binding of an inhibitor, and not simply a result of SKF86002 leaching out of the crystal, a Pim1 crystal was transferred into a fresh drop of well solution containing 10% DMSO (the solubilizing agent used for ligand screening) without SKF86002. The crystals were monitored after a 24 h incubation and a strong fluorescent signal was maintained (Fig. 5*d*). Three other compounds, P-017529, P-020547 and P-043305, which do not inhibit Pim1 kinase, were also used for soaking. Compared with the inhibitors quercetin and compound **1**, the crystals soaked with the non-inhibitory compounds retained their fluorescence indefinitely (Figs. 5*e*, 5*f* and 5*g*). We thus concluded that the decrease in the fluorescent signal is a result of competitive binding by the soaked compound.

3.3. Structures of the fluorescent SKF86002 complexes and the soaked and substituted inhibitor complexes of Pim1 and HCK

The structural determination of Pim1 co-crystallized in the presence of SKF86002 confirmed that the compound binds to the ATP-binding site. The electron density for SKF86002 was unambiguously assigned (Fig. 6*a*). The structures of the Pim1–SKF86002 complexes obtained by co-crystallization (refined to 2.0 Å resolution) or by soaking (data not shown) with SKF86002 (refined to 2.5 Å resolution) are identical, with an r.m.s.d. of 0.26 Å for 266 aligned C^{α} residues. This is important, as it shows that the compound binds in the same manner and the protein adopts the same conformation regardless of whether the complex is formed by co-crystallization or by soaking, despite the different crystallization conditions. These structures reflected those of other Pim1 complexes, with r.m.s.d.s of 0.36 and 0.42 Å compared with the kinase in complexes with myricetin (PDB entry 2o63; Holder *et al.*, 2007) and with p27(Kip1) carboxy-terminal peptide (PDB entry 3a99; Morishita *et al.*, 2011), respectively.

The SKF86002 compound does not form direct hydrogen-bonding interactions with the protein, which explains its low affinity and lack of specificity. However, it makes many hydrophobic interactions typical of other ATP-mimetic inhibitors.

The Pim1–SKF86002 co-crystals were soaked with the inhibitors quercetin and compound **1** and loss of the fluorescent signal was confirmed. Data sets were

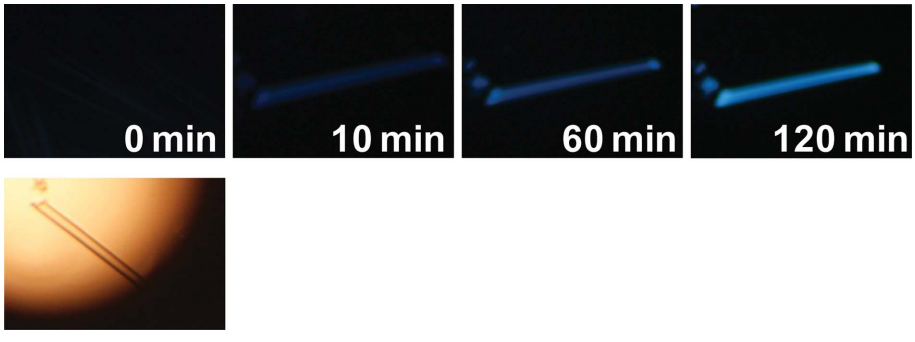

Figure 4
Apo Pim1 crystal soaked with SKF86002 (approximate crystal size 0.6 × 0.08 × 0.08 mm). An apo Pim1 crystal soaked with SKF86002 dihydrochloride produced increased fluorescent intensity upon binding of SKF86002 to the kinase. Data were obtained 0, 10, 60 and 120 min after the addition. Upper panels, images under UV illumination; lower panel, a white-light image.

then collected for two Pim1 co-crystals in which the SKF86002 was substituted by the inhibitors quercetin and compound **1** and were refined to 2.38 and 2.25 Å, respectively. In both cases, the electron density revealed that the inhibitors effectively replaced SKF86002 (Figs. 6*b* and 6*c*). The structure of our quercetin complex is almost identical to the previously reported quercetin-complex structure (PDB entry 2o3p), with an r.m.s.d. of 0.32 Å for 266 C^{α} atoms determined using *Coot* LSQ structure matching, and contains the typical hydrogen

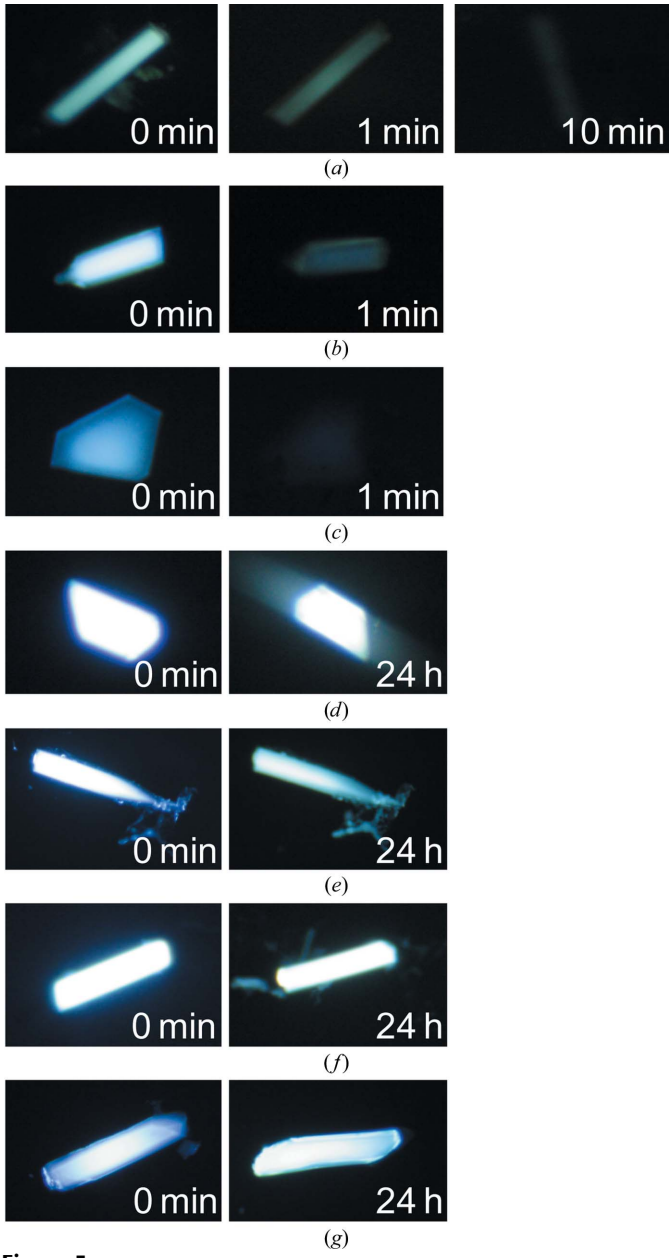

Figure 5
Inhibitor addition to SKF86002 co-crystals caused loss of fluorescence. (*a*) Pim1 co-crystals (approximate crystal size 0.6 × 0.08 × 0.08 mm) were soaked with quercetin. (*b*) Pim1–SKF86002 crystals (0.5 × 0.15 × 0.1 mm) were soaked with compound **1**. (*c*) HCK co-crystals (0.3 × 0.3 × 0.04 mm) were soaked with a final concentration of 2 m*M* A-419259. (*d*) A Pim1–SKF86002 crystal (0.4 × 0.3 × 0.2 mm) was transferred into well solution with 10% DMSO. (*e*)–(*g*) Pim1–SKF86002 crystals soaked with 1 m*M* (*e*) P-017529 (approximate crystal size 0.6 × 0.15 × 0.15 mm), (*f*) P-020547 (0.6 × 0.15 × 0.15 mm) and (*g*) P-043305 (0.6 × 0.15 × 0.15 mm). Images were obtained under UV illumination. Photographs were taken at the indicated times after soaking.

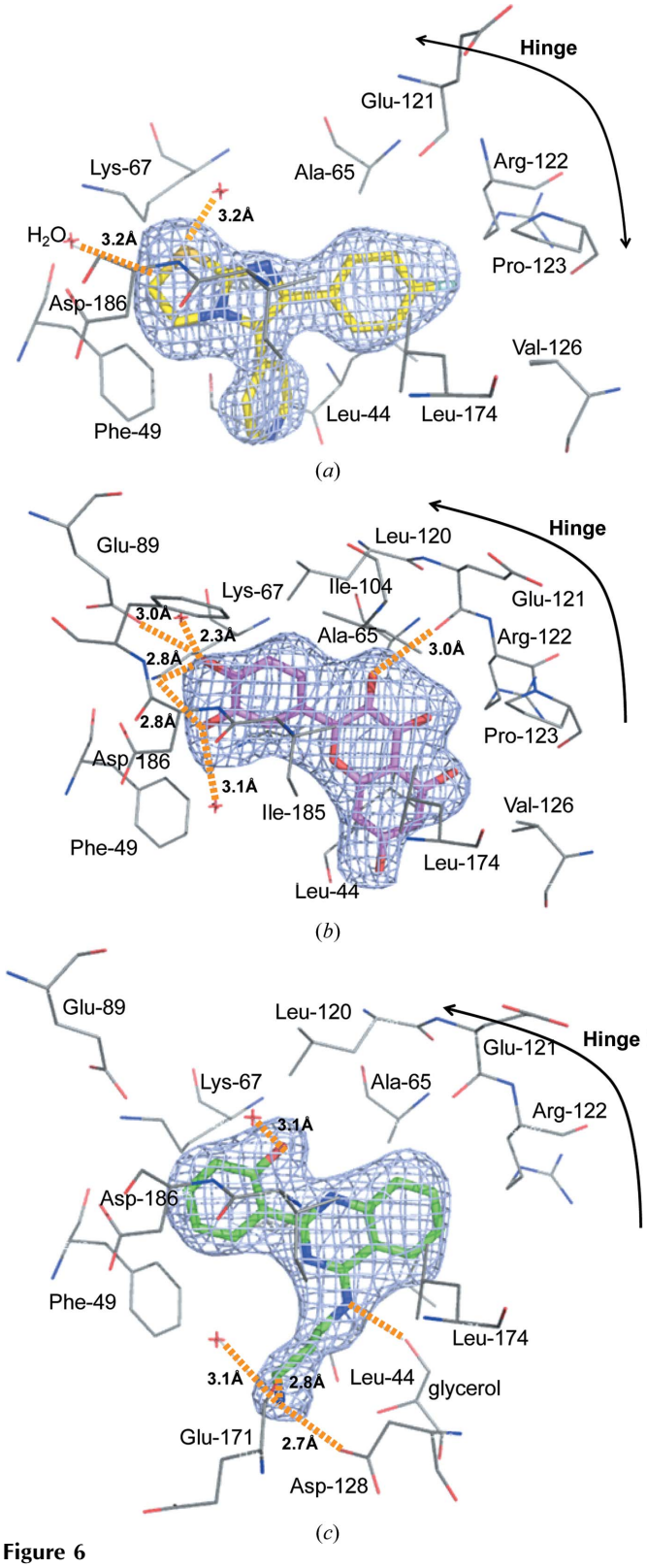

Figure 6
Interactions between Pim1 and ligands. (*a*) Pim1–SKF86002, (*b*) Pim1–quercetin and (*c*) Pim1–compound **1**. The side chains of residues that interact with the compound are shown as grey lines. Orange dotted lines depict hydrogen bonds.

bonds formed to Glu89, Lys67 and Glu121. As expected, the compound **1** structure is also identical to that previously reported (Tsuganezawa *et al.*, 2012; PDB entry 3uix), with an r.m.s.d. of 0.13 Å for 256 C^{α} atoms. The quercetin and compound **1** molecules were refined to 100% occupancy, with average *B* factors of 55.77 and 34.91 Å^2, respectively. The structure of Pim1 complexed with SKF86002 was superimposed with those with quercetin and compound **1** (Figs. 7*a* and 7*b*) to show the locations of the inhibitors compared with that of the SKF86002 molecule prior to displacement.

The structures of HCK in complexes with SKF86002 and the inhibitor A-419259 were refined to 2.85 and 3.04 Å resolution, respectively (Figs. 8*a* and 8*b*). The electron density for the SKF86002 molecule was evident immediately after molecular replacement. The SKF86002 molecule in the HCK complex binds in a different orientation to that observed in the Pim1 structures. This is presumably owing to the different binding-site compositions between the two kinases: the back of the ATP-binding pocket in Pim1 includes larger and more hydrophobic residues than that in HCK. SKF86002 forms many hydrophobic interactions with the hinge region of HCK, as well as a hydrogen bond to the backbone carbonyl and amine of the methionine residue in this region. This is not observed in Pim1, since Pim1 has a unique hinge region with a proline residue at this position. The HCK A-419259-soaked structure revealed unambiguous electron density for the large inhibitor, confirming that the fluorescent SKF86002 molecule is displaced in the soaked and non-fluorescent crystal. This structure is identical to the recently deposited crystal structure of the same complex (PBD entry 3vs3; Saito *et al.*, 2013), with

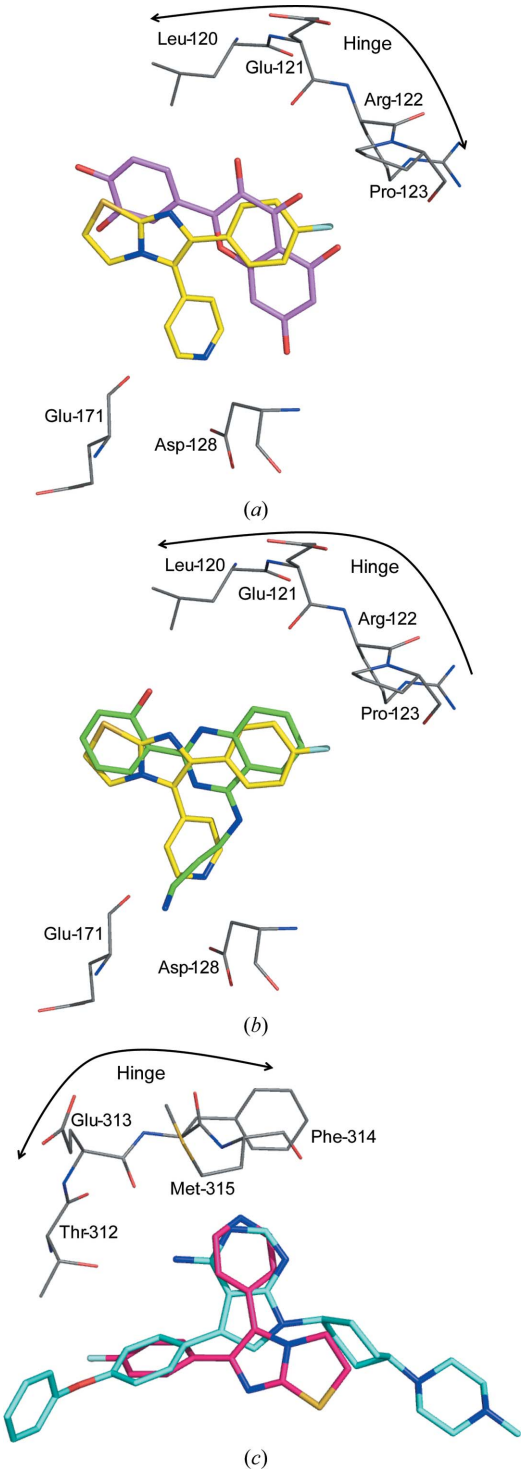

Figure 7
Overlay of the ligands binding to kinases. (*a*) SKF86002 and quercetin complexed with Pim1, (*b*) SKF86002 and compound **1** complexed with Pim1 and (*c*) SKF86002 and A-419259 complexed with HCK. The hinge residues are shown for orientation.

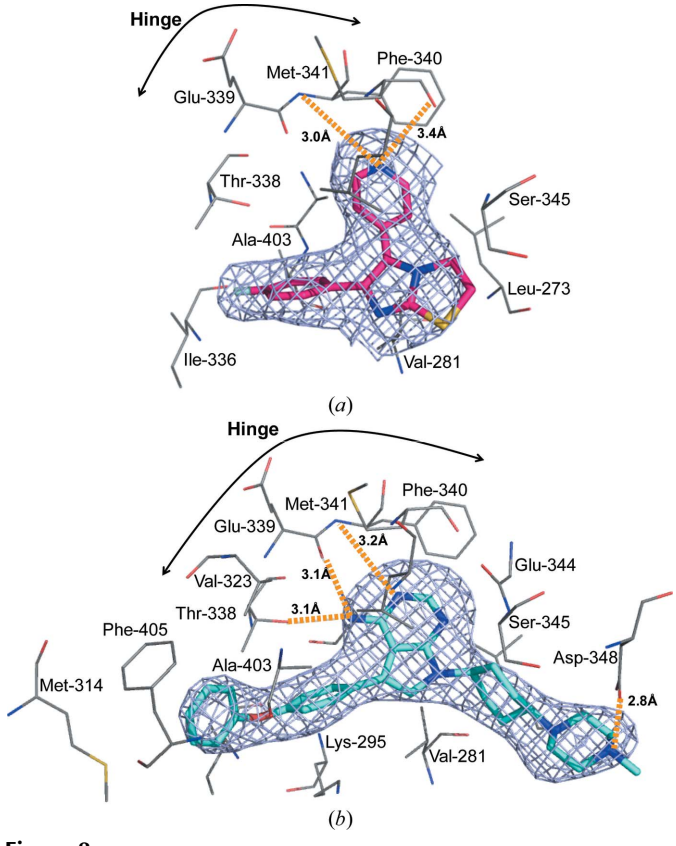

Figure 8
Interactions between HCK and ligands. (*a*) HCK–SKF86002 and (*b*) HCK–A-419259. The side chains of residues that interact with the compound are shown as grey lines. Orange dotted lines depict hydrogen bonds.

Table 2
KINOME*scan* results.

Entrez gene symbol	KINOME*scan* gene symbol	Kinase–SKF86002 complex (%)
ABL1	ABL1(E255K)-phosphorylated	72
ABL1	ABL1(T315I)-phosphorylated	38
ABL1	ABL1-nonphosphorylated	0
ABL1	ABL1-phosphorylated	43
ACVR1B	ACVR1B	99.1
AKT1	AKT1	68
AKT2	AKT2	76
ALK	ALK	98.6
AURKA	AURKA	0
AURKB	AURKB	25
AXL	AXL	97.2
BMPR2	BMPR2	64
BRAF	BRAF	95.5
BRAF	BRAF(V600E)	96.8
BTK	BTK	14
CABC1	ADCK3	100
CDK16	PCTK1	6
CDK19	CDK11	94.7
CDK2	CDK2	54
CDK3	CDK3	52
CDK7	CDK7	55
CDK9	CDK9	20
CHEK1	CHEK1	47
CHUK	IKK-alpha	0
CSF1R	CSF1R	82
CSNK1D	CSNK1D	99.6
CSNK1G2	CSNK1G2	100
DCLK1	DCAMKL1	26
DYRK1B	DYRK1B	68
EGFR	EGFR	99.6
EGFR	EGFR(L858R)	99.7
EPHA2	EPHA2	91.6
ERBB2	ERBB2	71
ERBB4	ERBB4	97.5
FGFR2	FGFR2	70
FGFR3	FGFR3	59
FLT3	FLT3	90.8
GSK3B	GSK3B	89
IGF1R	IGF1R	58
IKBKB	IKK-beta	0
INSR	INSR	64
JAK2	JAK2(JH1domain-catalytic)	0
JAK3	JAK3(JH1domain-catalytic)	0
KDR	VEGFR2	72
KIT	KIT	95.2
KIT	KIT(D816V)	95.6
KIT	KIT(V559D,T670I)	74
MAP2K1	MEK1	87
MAP2K2	MEK2	94
MAP3K4	MAP3K4	73
MAP3K9	MLK1	56
MAPK10	JNK3	99.5
MAPK11	p38-beta	100
MAPK14	p38-alpha	100
MAPK3	ERK1	80
MAPK8	JNK1	99.8
MAPK9	JNK2	99.8
MAPKAPK2	MAPKAPK2	0
MARK3	MARK3	72
MET	MET	98.2
MKNK1	MKNK1	37
MKNK2	MKNK2	95.5
NTRK1	TRKA	12
NUAK2	SNARK	62
PAK1	PAK1	93.6
PAK2	PAK2	84
PAK4	PAK4	44
PDGFRA	PDGFRA	45
PDGFRB	PDGFRB	98.8
PDPK1	PDPK1	37
PIK3C2B	PIK3C2B	68
PIK3CA	PIK3CA	1
PIK3CG	PIK3CG	43
PIM1	PIM1	98.8
PIM2	PIM2	98.3
PIM3	PIM3	95.6
PLK1	PLK1	45
PLK3	PLK3	28
PLK4	PLK4	1
PRKACA	PKAC-alpha	99.9
PRKCE	PRKCE	0
PTK2	FAK	74
RAF1	RAF1	95.2
RET	RET	87
RIOK2	RIOK2	60
ROCK2	ROCK2	69
RPS6KA3	RSK2(Kin.Dom.1-N-terminal)	87
SRC	SRC	99
SRPK3	SRPK3	76
STK11	LKB1	0
STK32C	YANK3	93.8
TEK	TIE2	86
TGFBR1	TGFBR1	99.7
TSSK1B	TSSK1B	54
TYK2	TYK2(JH1domain-catalytic)	0
ULK2	ULK2	5
ZAP70	ZAP70	59

an r.m.s.d. of 0.375 Å for 837 C^{α} atoms. The structures of HCK in complex with SKF86002 and with A-419259 were superimposed (Fig. 7*c*) to show the location of the inhibitor compared with that of the SKF86002 molecule prior to displacement.

Kinase inhibition assays revealed that SKF86002 did not inhibit Pim1 and HCK, even at 100 µ*M*, and only weakly inhibited AMPK. Presumably, the high concentrations of ATP molecules in the kinase assay mixtures competed with SKF86002 and therefore no inhibition was observed. Although inhibition was not detected, the crystal structures revealed that SKF86002 does bind to the ATP-binding sites of both Pim1 and HCK, and thus presumably also to the site in AMPK.

A comparison of the p38α–SKF86002 structure (PDB entry 1oz1; Trejo *et al.*, 2003) with our Pim1 and HCK complex structures shows that the diarylimidazole inhibitor bound to p38α adopts a very similar orientation to SKF86002 in the HCK complex. The inhibitor makes a hydrogen bond to the main-chain amide N atom of residue 109 in p38α. This hydrogen bond is observed between SKF86002 and the main-chain amide N atom of residue 315 in the HCK–SKF86002 complex, so we predict that the same interaction may form when SKF-86002 interacts with p38α. Furthermore, superposition of the HCK–SKF86002 structure with AMPK (PDB entry 2y94; Xiao *et al.*, 2011) suggests that the same hydrogen bond may be formed with the main-chain amide of residue 96. On the other hand, Pim1 does not make a hydrogen bond to SKF-86002. This kinase is unique as it has a proline residue at position 123 and is thus unable make this hydrogen bond to the inhibitor. The loss of the hydrogen bond in the Pim1

complex might be a contributing factor in the low fluorescence intensity observed in Fig. 2.

3.4. Wide application of SKF86002 as a kinase crystal marker

To investigate the potential of SKF86002 as a general kinase crystal marker, we assessed its binding to 97 kinases, including important mutants, in the kinome dendrogram. In the assay, kinase active-site-directed ligands were immobilized on a chip and the amount of kinase that bound to the ligands on the chip was measured. The binding assay was performed in the presence of SKF86002. The interaction of SKF86002 with each target kinase competitively decreased the interaction between the kinase and the ligands on the chip, and thus decreased the amount of kinase bound to the chip. Owing to experimental limitations, we used a final concentration of 0.8 m*M* SKF86002 for the assay, which was rather low compared with that employed for co-crystallization. However, among the 97 kinases tested, SKF86002 bound strongly to 68 kinases (Fig. 9, large and medium red circles) as follows: ABL1(E255K)-phosphorylated, ACVR1B, AKT1, AKT2, ALK, AXL, BMPR2, BRAF, BRAF(V600E), CABC1, CDK2, CDK3, CDK7, CDK19, CSF1R, CSNK1D, CSNK1G2, DYRK1B, EGFR, EFGF(L858R), EPHA2, ERBB2, ERBB4, FGFR2, FGFR3, FLT3, GSK3B, IGF1R, INSR, KDR, KIT, KIT(D816V), KIT(V559D,T670I), MAP2K1, MAP2K2, MAP3K4, MAP3K9, MAPK3, MAPK8, MAPK9, MAPK10, MAPK11, MAPK14, MARK3, MET, MKNK2, NUAK2, PAK1, PAK2, PDGFRB, PIK3C2B, PIM1, PIM2, PIM3, PRKACA, PTK2, RAF1, RET, RIOK2, ROCK2, PRS6KA3, SRC, SRPK3, STK32C, TEK, TGFBR1, TSSK1B and ZAP70 (Entrez gene symbols; Table 2). SKF86002 did not bind at all to ABL1-nonphosphorylated, AURKA, CHUK, IKBKB, JAK2, JAK3, MAPKAPK2, PRKCE, STK11 and TYK2 (Table 2). We thus concluded that this kinase probe may be applicable to a fairly wide range of kinases. Even if inhibition of a kinase by SKF86002 is not observed, as in the cases of Pim1 and HCK, SKF86002 might still effectively bind to it and be a useful probe for inhibitor screening. The saturation concentration of SKF86002 dihydrochloride in water is as high as 50 m*M*, and free SKF86002 is not fluorescent. Thus, we presume that many kinases will bind to SKF860002 and become fluorescent when it is added at higher concentrations to crystallization buffers.

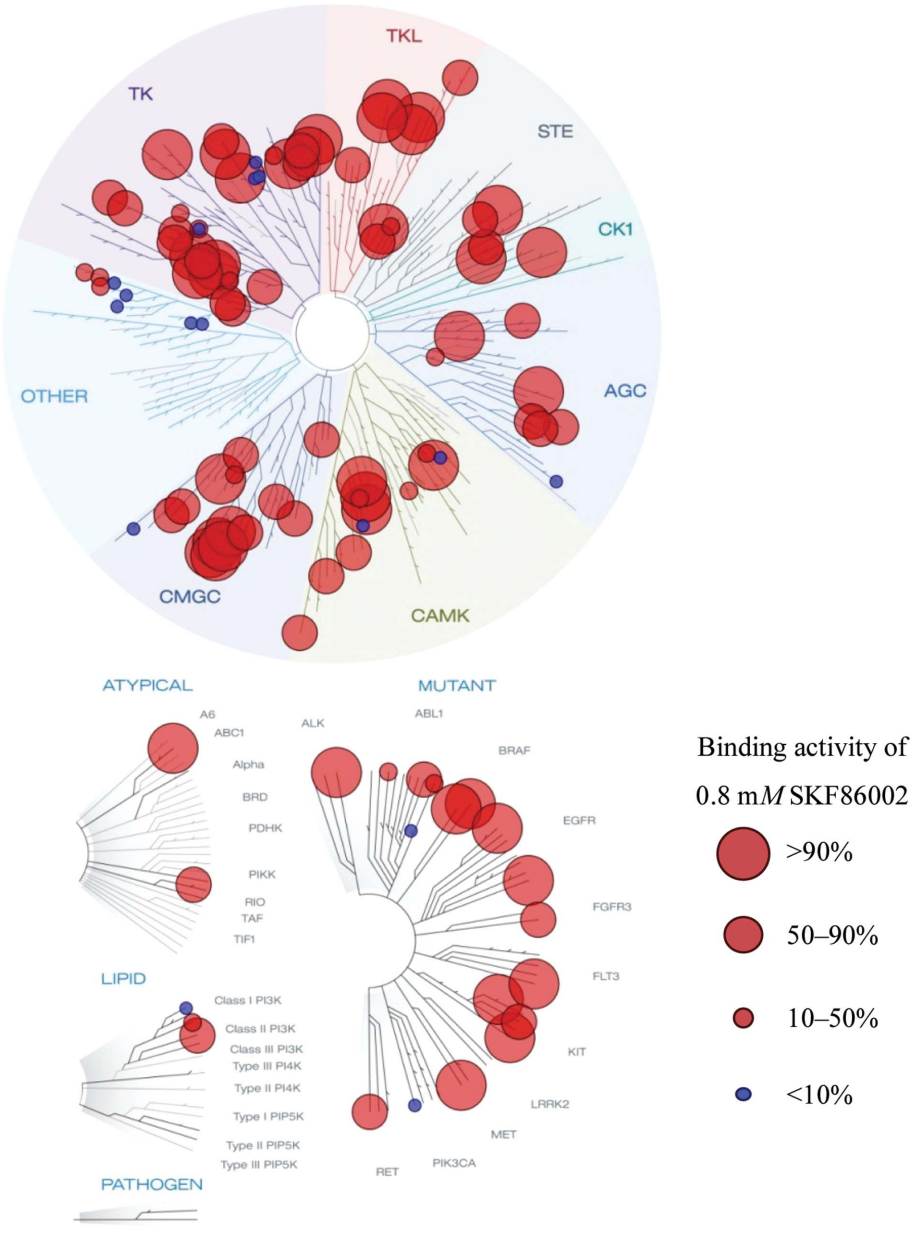

Figure 9
Kinase dendrogram. Binding activities of 0.8 m*M* SKF86002 with 97 kinases, as determined using KINOME*scan* technology. The 68 kinases that bound strongly to SKF86002 are indicated by medium and large red circles.

4. Discussion

During the last decade, crystallography has become commonly employed as the primary assay tool for compound screening, and it is now recognized as one of the most sensitive assay techniques in fragment screening. Unlike many other biophysical techniques, crystallography is able to detect compounds with binding affinities in the millimolar range. Our method differs from traditional screening as it uses SKF86002 co-crystals for screening rather than apo crystals. We showed

that screening can be performed with larger compounds, instead of relatively small fragments. This technique also filters out compounds with affinities lower than that of SKF86002 and confirms, prior to structure determination, that the compound has bound through the loss of crystal fluorescence. The ease and speed at which we can, in theory, subsequently solve the structure of the complex, thanks to highly automated structure determination, and progress straight to inhibitor optimization using the obtained structural details are some of the main advantages of our method. In traditional fragment screening, actual confirmation of compound binding is only possible after data collection and structure determination. Our technique allows the specific selection of only those crystals with bound inhibitors by checking for the loss of the fluorescent signal, and thus saves significant time, effort and cost.

Using Pim1, we have proved that our strategy can successfully differentiate between compounds that bind to the ATP site and compounds that do not bind at all. The structures of Pim1 and HCK with SKF86002 confirmed that the compound binds to the ATP site, as predicted. Further experimentation using larger sets of compounds is required to test the efficacy of the inhibitor-screening technique with SKF86002–kinase co-crystals, but our preliminary results suggested that this will be straightforward. Additionally, further research is required to explore the utility of this technique with other kinases. However, as suggested by the kinome assay and the preliminary results with Pim1 and HCK, at least a significant group of protein kinases can be screened using the SKF86002 fluorescence technique described here.

There are naturally some obvious drawbacks of this technique, especially those associated with using soaking, as opposed to co-crystallization, for complex formation. The successful soaking of compounds into previously formed crystals may be limited by binding-site accessibility. Generally, compounds use solvent channels to traverse to the binding site. In a crystal, these channels may be too narrow or completely blocked, especially if the compound is relatively large. This could result in false-negative results. Furthermore, in the soaking screening step, major conformational changes upon compound binding may be prevented from occurring as a consequence of the rigidity and restricted movement owing to crystal contacts. These conformational changes may be permitted in solution and thus observed in co-crystallized complexes. Although these limitations are common problems associated with complex formation using the soaking technique, rather than co-crystallization, soaking is still often employed for structural studies of many complexes. It is notable that despite the rigidity imposed by the pre-formed crystals, flexibility around the binding site, flipping of loops and other significant conformational changes in protein crystals are frequently observed (Gill *et al.*, 2005; Hartshorn *et al.*, 2005; Bosch *et al.*, 2006; Verlinde *et al.*, 2009; Raghunathan *et al.*, 2010; Parker *et al.*, 2012; Chilingaryan *et al.*, 2012). Although co-crystallization is generally the preferred technique, soaking ligands into crystals can produce excellent and informative results, as long as the regions involved in the binding site do not form crystal contacts. The structures obtained from co-crystallization often reflect those acquired using the soaking technique. Indeed, our Pim1–quercetin structure obtained by soaking quercetin into an SKF86002 co-crystal is essentially identical to the previously reported Pim1-quercetin structure (Holder *et al.*, 2007), which was determined by co-crystallization with quercetin. Furthermore, our two Pim1–SKF86002 structures obtained by soaking and co-crystallization are identical to each other. The HCK–A-419259 structure reported here, produced by soaking the inhibitor into an HCK–SKF86002 co-crystal, is identical to another recently deposited HCK–A-419259 structure (PDB entry 3vs3) which was obtained by co-crystallizing HCK with an alternative inhibitor and then soaking it with A-419259. The HCK structure seems to be the same whether it is co-crystallized with SKF86002 or a totally different inhibitor.

One of the most convenient aspects of this technique is that data can be collected directly from the crystals used in the screening stage. The observed decrease in the fluorescent signal allows us to rapidly identify crystals in which a compound has bound to the ATP site. In contrast, other techniques require data collection and structure determination before this can be confirmed. Additionally, this technique identifies compounds that bind specifically to the ATP-binding site, while some other techniques produce false positives as they are unable to differentiate the binding site.

5. Conclusions

We have reported the development, validation and implementation of a novel screening method that assists in protein crystal identification and facilitates inhibitor screening in the structure-based drug-discovery process.

We have shown that two essential steps in inhibitor development can be simplified by incubating the protein with just one compound prior to crystallization. SKF86002 dihydrochloride, which is water-soluble, avoids the use of harsher solubilizing agents such as DMSO, which can be counterproductive in crystal growth. The fluorescent signal generated by the kinase–SKF86002 co-crystals assists in straightforward protein kinase crystal identification and facilitates inhibitor screening by allowing rapid identification and confirmation of compound binding. This technique may be applied to a significant number of kinases and may even assist in the crystallization of kinases that otherwise would not crystallize easily in the apo form. Further investigations of the usefulness of this technique are currently under way and our preliminary results have shown that other kinases can be successfully screened using SKF86002 dihydrochloride.

This work was supported in part by the Targeted Protein Research Programs from the Ministry of Education, Culture, Sports, Science and Technology of Japan. LJP was supported by a National Health and Medical Research Council of Australia (NHMRC) CJ Martin Overseas Postdoctoral Fellowship and a Start-Up grant from the Ministry of Education, Culture, Sports, Science and Technology of Japan.

We also thank the beamline staff of the MX2 (Australian Synchrotron) and BL26B2 (SPring-8) beamlines and T. Umehara, H. Niwa and R. Akasaka (RIKEN) for help in X-ray data collection.

References

Adams, P. D. *et al.* (2010). *Acta Cryst.* D**66**, 213–221.
Anastassiadis, T., Deacon, S. W., Devarajan, K., Ma, H. & Peterson, J. R. (2011). *Nature Biotechnol.* **29**, 1039–1045.
Bosch, J. *et al.* (2006). *J. Med. Chem.* **49**, 5939–5946.
Bunkoczi, G., Salah, E., Filippakopoulos, P., Fedorov, O., Müller, S., Sobott, F., Parker, S. A., Zhang, H., Min, W., Turk, B. E. & Knapp, S. (2007). *Structure*, **15**, 1215–1226.
Burchat, A., Borhani, D. W., Calderwood, D. J., Hirst, G. C., Li, B. & Stachlewitz, R. F. (2006). *Bioorg. Med. Chem. Lett.* **16**, 118–122.
Chilingaryan, Z., Yin, Z. & Oakley, A. J. (2012). *Int. J. Mol. Sci.* **13**, 12857–12879.
Diskin, R., Lebendiker, M., Engelberg, D. & Livnah, O. (2007). *J. Mol. Biol.* **365**, 66–76.
Emsley, P. & Cowtan, K. (2004). *Acta Cryst.* D**60**, 2126–2132.
Fabian, M. A. *et al.* (2005). *Nature Biotechnol.* **23**, 329–336.
Forsythe, E., Achari, A. & Pusey, M. L. (2006). *Acta Cryst.* D**62**, 339–346.
Gallagher, T. F. *et al.* (1997). *Bioorg. Med. Chem.* **5**, 49–64.
Gill, A. L. *et al.* (2005). *J. Med. Chem.* **48**, 414–426.
Groves, M. R., Müller, I. B., Kreplin, X. & Müller-Dieckmann, J. (2007). *Acta Cryst.* D**63**, 526–535.
Handa, N. *et al.* (2011). *Acta Cryst.* D**67**, 480–487.
Hartshorn, M. J., Murray, C. W., Cleasby, A., Frederickson, M., Tickle, I. J. & Jhoti, H. (2005). *J. Med. Chem.* **48**, 403–413.
Holder, S., Zemskova, M., Zhang, C., Tabrizizad, M., Bremer, R., Neidigh, J. W. & Lilly, M. B. (2007). *Mol. Cancer Ther.* **6**, 163–172.
Judge, R. A., Swift, K. & González, C. (2005). *Acta Cryst.* D**61**, 60–66.
Lantos, I., Bender, P. E., Razgaitis, K. A., Sutton, B. M., DiMartino, M. J., Griswold, D. E. & Walz, D. T. (1984). *J. Med. Chem.* **27**, 72–75.
Laskowski, R. A., MacArthur, M. W., Moss, D. S. & Thornton, J. M. (1993). *J. Appl. Cryst.* **26**, 283–291.
McCoy, A. J., Grosse-Kunstleve, R. W., Adams, P. D., Winn, M. D., Storoni, L. C. & Read, R. J. (2007). *J. Appl. Cryst.* **40**, 658–674.
Morishita, D., Takami, M., Yoshikawa, S., Katayama, R., Sato, S., Kukimoto-Niino, M., Umehara, T., Shirouzu, M., Sekimizu, K., Yokoyama, S. & Fujita, N. (2011). *J. Biol. Chem.* **286**, 2681–2688.
Nakano, H., Saito, N., Parker, L. J., Tada, Y., Abe, M., Tsuganezawa, K., Yokoyama, S., Tanaka, A., Kojima, H., Okabe, T. & Nagano, T. (2012). *J. Med. Chem.* **55**, 5151–5164.
Pargellis, C., Tong, L., Churchill, L., Cirillo, P. F., Gilmore, T., Graham, A. G., Grob, P. M., Hickey, E. R., Moss, N., Pav, S. & Regan, J. (2002). *Nature Struct. Biol.* **9**, 268–272.
Parker, L. J., Watanabe, H., Tsuganezawa, K., Tomabechi, Y., Handa, N., Shirouzu, M., Yuki, H., Honma, T., Ogawa, N., Nagano, T., Yokoyama, S. & Tanaka, A. (2012). *Acta Cryst.* F**68**, 860–866.
Pene-Dumitrescu, T., Peterson, L. F., Donato, N. J. & Smithgall, T. E. (2008). *Oncogene*, **27**, 7055–7069.
Raghunathan, K., Harris, P. T. & Arvidson, D. N. (2010). *Acta Cryst.* F**66**, 615–620.
Saito, Y. *et al.* (2013). *Sci. Trans. Med.* **5**, 181ra152.
Schindler, T., Sicheri, F., Pico, A., Gazit, A., Levitzki, A. & Kuriyan, J. (1999). *Mol. Cell*, **3**, 639–648.
Sicheri, F., Moarefi, I. & Kuriyan, J. (1997). *Nature (London)*, **385**, 602–609.
Trejo, A. *et al.* (2003). *J. Med. Chem.* **46**, 4702–4713.
Tsuganezawa, K. *et al.* (2012). *J. Mol. Biol.* **417**, 240–252.
Verlinde, C. L. *et al.* (2009). *Curr. Top. Med. Chem.* **9**, 1678–1687.
Xiao, B. *et al.* (2011). *Nature (London)*, **472**, 230–233.